

Topological Susceptibility in the Superconductive Phases of Quantum Chromodynamics: a Dyson-Schwinger Perspective

Fabrizio Murgana,^{1,2,*} Giorgio Comitini,^{1,2,†} and Marco Ruggieri^{1,2,‡}

¹*Department of Physics and Astronomy "Ettore Majorana",
University of Catania, Via Santa Sofia 64, I-95123 Catania, Italy*
²*INFN-Sezione di Catania, Via Santa Sofia 64, I-95123 Catania, Italy*

We test non-perturbative gluon propagators recently studied in the literature, by computing the topological susceptibility, χ , of the superconductive phases of Quantum Chromodynamics at high density. We formulate the problem within the High-Density Effective Theory, and use the 2-particle irreducible formalism to compute the effective potential of the dense phases. We focus on superconductive phases with two and three massless flavors. Within this formalism, we write a Dyson-Schwinger equation in the rainbow approximation for the anomalous part of the quark propagator in the superconductive phases, in which the non-perturbative gluon propagator plays its role. We complete the model by adding a $U(1)_A$ -breaking term whose coupling is fixed perturbatively at large quark chemical potential. We then use the effective potential to compute χ in the superconductive phases. We finally discuss implications of the results for the axion mass in superdense phases of Quantum Chromodynamics.

PACS numbers: 12.38.Aw,12.38.Mh

Keywords: QCD, Topological susceptibility, CJT formalism, HDET

I. INTRODUCTION

The theory of strong interactions, Quantum Chromodynamics (QCD), can be augmented by a term that does not break gauge invariance, but which is odd under parity as well as under the combined operations of parity and charge conjugation. This term is topological in nature and can be written as

$$S_\theta = \theta \int d^4x q(x), \quad (1)$$

where θ is a real number sometimes called the θ -angle of QCD, $q(x)$ is the topological charge density,

$$q(x) = \frac{g^2}{64\pi^2} \epsilon^{\mu\nu\rho\sigma} F_{\mu\nu}^a F_{\rho\sigma}^a, \quad (2)$$

and $F_{\mu\nu}^a$ denotes the field strength tensor of the gluon field. Through a Fujikawa transformation, the θ -term can be reabsorbed into the quark sector, introducing an anomalous phase in the quark mass term which ultimately leads to the explicit breaking of the $U(1)_A$ symmetry. In the framework of the instanton liquid model, this breaking is associated with an effective multi-fermion interaction among quarks due to instanton exchange.

In the context of QCD at finite θ , it is useful to introduce the topological susceptibility, χ , defined as the second derivative of the effective potential of QCD with respect to θ at $\theta = 0$. χ quantifies the fluctuations of the topological charge in QCD. This quantity has been extensively studied in the vacuum and at finite temperature,

both within effective models [1–5], as well as with χ PT [6–9] and in Lattice QCD simulations [10–12]. However, studies of χ at finite chemical potential remain scarce, mainly due to the sign problem in Lattice QCD. In particular, very little is known about the behavior of topological fluctuations in the color-superconducting phase of QCD, where the formation of diquark condensates and the modification of the axial anomaly could significantly impact the topological sector of the theory.

In this work, we compute χ in superdense phases of QCD, in which the system could be in a color-superconductive phase [13–25]. We make use of a renormalized version of QCD around the Fermi surface of quarks, known as High Density Effective Theory (HDET), see [16] for a review. In our work, we combine HDET with a non-local Dyson-Schwinger equation (DSE) for the quark propagator in the rainbow approximation (bare vertices) supplemented with improved gluon propagators [26]. We derive the relevant DSE within the 2-particle-irreducible (2PI) formalism of Cornwall-Jackiw-Toumboulis (CJT) [27]. This requires the formulation of dense QCD at finite θ , which has not been studied within the aforementioned approach yet. The propagators of [26] have been used so far only to get a semi-quantitative picture of the QCD phase diagram, but have not been used in calculations of QCD properties like condensates, susceptibilities and so on. Therefore, with this work we offer a first test of their impact on the QCD condensates and on the QCD thermodynamic potential.

Several studies have been carried out in the DSE framework for the color superconductive phases, see for example [17, 28–32]. Compared to these studies, in this work we write a DSE for the quark propagator within the HDET formalism, and use an improved gluon propagator which was recently obtained in [26], that entails

* fabrizio.murgana@dfa.unict.it

† giorgio.comitini@dfa.unict.it

‡ marco.ruggieri@dfa.unict.it

non-perturbative screening masses.

In order to compute the topological susceptibility, we include an explicit $U_A(1)$ breaking term [33, 34] which effectively describes the one-instanton exchange (OIE) among quarks, as well as their coupling to the θ -angle when a standard Fujikawa rotation is performed to remove the parity-odd term (1) from the QCD Lagrangian. This term has already been used in effective models with a contact interaction [1–4, 35–37], in combination with an effective coupling describing the one-gluon exchange (OGE). In this work, rather than embracing the approach of local effective models, we start with the full QCD Lagrangian, renormalize it around the Fermi surface isolating only the relevant terms at large μ , then we add the OIE at finite θ . The dependence of the coupling in the OIE channel, ζ , on the quark chemical potential, μ , and the QCD coupling, g , is fixed by its perturbative expression at large μ , both in the two-flavor and in the three-flavor models we consider.

One of the potential applications of this work is the study of the QCD-axion [37–40] in dense QCD phases. In fact, the axion potential is directly accessible from the QCD potential at finite θ by the formal replacement $\theta \rightarrow a/f_a$ where a denotes the axion field and f_a is the axion decay constant. Hence, the calculation of the effective QCD potential at finite θ allows us to access the low-energy properties of the axion, like the mass, the self-coupling and so on. We will comment briefly on the impact of our results on the axion mass in Section VII, leaving a more complete study of this interesting problem to future works.

The plan of the article is as follows. In Section II we summarize the HDET and the 2PI formalisms adapted to the CFL phase, as well as the gluon propagator we use in the DSE. In Section III we derive the HDET gap equation within the HDET. In Section IV we present the gap equation for the CFL phase, and set the basic relations that help to write the topological susceptibility in a compact form. In Section V we discuss our calculation of the topological susceptibility of the CFL phase. In Section VI we briefly discuss the topological susceptibility of the 2SC phase. In Section VII we discuss semi-analytical relations between χ and the couplings of the model in two limiting cases. In Section VIII we comment on the relevance of our results for the computation of the QCD axion mass in color-superconductive phases. Finally, in Section IX we present our conclusions and an outlook. We use $\hbar = c = 1$ throughout the article.

II. MODEL AND CALCULATION SETUP

A. HDET for color-superconductive phases

The High-Density Effective Theory (HDET) is a very well established framework for the study of strongly interacting matter under conditions of extremely high density [16, 41–43]. It provides a systematic method to explore

these regimes by focusing on the degrees of freedom most relevant at high baryon density, significantly simplifying the calculations but still effectively capturing the high-density behavior of the theory. The HDET has been used to study the properties of color-superconducting phases, allowing for semi-analytical calculations of the gap parameters and critical temperatures for various pairing patterns [15, 23, 35, 41, 44–53]. Recently, it has also been used to construct an effective model to describe the quark-condensation pattern on the Fermi surface [54]. By focusing on the Fermi surface dynamics, HDET can also provide insight into the equation of state (EoS) of dense matter, a critical ingredient for modeling neutron stars and other compact astrophysical objects [16, 41]. Furthermore, HDET has been used to elucidate the properties of collective excitations, such as Nambu-Goldstone bosons arising from symmetry breaking in dense QCD phases [23].

The HDET of QCD is well known, therefore we limit ourselves to summarize the main ideas of the formulation; for more details, we refer to [16]. The key idea behind HDET is that at $T = 0$, the vacuum is characterized by fermions filling all available low-energy states up to the Fermi energy. Due to the Pauli exclusion principle, interactions involving low-energy quarks necessarily involve the exchange of high-momentum particles. This is suppressed in QCD because of asymptotic freedom. Consequently, the leading contribution to the thermodynamic properties of dense QCD comes from the quarks near the Fermi surface. Thus, the effective Lagrangian in HDET is constructed by expanding around the Fermi surface and including only terms that are relevant close to the Fermi surface. The resulting theory describes quasi-particles and their interactions, thus providing a framework to analyze the pairing mechanisms and gap structures.

In the HDET, the quark momenta are decomposed as

$$p^\mu = \mu v^\mu + \ell^\mu, \quad (3)$$

where μ denotes the quark chemical potential, and $v^\mu = (0, \mathbf{v})$ with \mathbf{v} is the Fermi velocity vector, $|\mathbf{v}| = 1$. ℓ^μ is called the residual momentum, whose spatial part is

$$\boldsymbol{\ell} = \mathbf{v} \ell_{\parallel} + \boldsymbol{\ell}_{\perp}, \quad (4)$$

Here, ℓ_{\parallel} and ℓ_{\perp} correspond to the parallel and perpendicular components of the residual momentum. However, one can always choose the velocity parallel to \mathbf{p} , so that $\ell_{\perp} = 0$. The 4-integral measure of the HDET reads

$$\int \frac{d^4 p}{(2\pi)^4} = \frac{4\pi \mu^2}{(2\pi)^4} \sum_{\mathbf{v}} \int_{-\infty}^{+\infty} d\ell_{\parallel} \int_{-\infty}^{+\infty} d\ell_0. \quad (5)$$

with

$$\sum_{\mathbf{v}} \equiv \int \frac{d\mathbf{v}}{8\pi} = \frac{1}{2} \int \frac{d\phi_{\mathbf{v}} d\theta_{\mathbf{v}}}{4\pi}, \quad (6)$$

where (ϕ_v, θ_v) correspond to the azimuthal and polar angles of the Fermi velocity, and an additional factor $1/2$ is included in order to avoid double counting.

The leading-order HDET lagrangian density is

$$\mathcal{L}_{QCD}^{HDET} = \mathcal{L}_g + \mathcal{L}_D, \quad (7)$$

where

$$\mathcal{L}_g = -\frac{1}{4} F_{\mu\nu}^a F^{a\mu\nu} \quad (8)$$

is the standard gluon term, and

$$\mathcal{L}_D = \mathcal{L}_0 + \mathcal{L}_1 \quad (9)$$

is the quark Lagrangian. In Eq. (9), \mathcal{L}_0 represents the free Dirac Lagrangian, which in our framework can be written as

$$\mathcal{L}_0 = \sum_{\vec{v}} \left(\psi_+^\dagger iV \cdot \partial \psi_+ + \psi_-^\dagger i\tilde{V} \cdot \partial \psi_- \right) \quad (10)$$

while \mathcal{L}_1 represents the interaction term with the gluon field A ,

$$\mathcal{L}_1 = ig \sum_{\vec{v}} \left(\psi_+^\dagger iV \cdot A \psi_+ + \psi_-^\dagger i\tilde{V} \cdot A \psi_- \right) \quad (11)$$

Here $V = (1, \mathbf{v})$, $\tilde{V} = (1, -\mathbf{v})$, with \mathbf{v} being the aforementioned quark Fermi velocity, and ψ_\pm indicate the positive-energy velocity-dependent fields with opposite velocity

$$\psi_\pm \equiv \psi_{+, \pm \mathbf{v}}. \quad (12)$$

We include an additional term, \mathcal{L}_4 , in the Lagrangian density (7), that explicitly breaks $U(1)_A$ symmetry and describes the interaction among quarks due to the one-instanton exchange. Following [35], we take

$$\begin{aligned} \mathcal{L}_4 = & -\zeta \left[(\psi_L^T iC \psi_L) (\psi_R^\dagger iC \psi_R^*) e^{i\theta} \right. \\ & \left. + (\psi_R^T iC \psi_R) (\psi_L^\dagger iC \psi_L^*) e^{-i\theta} \right], \end{aligned} \quad (13)$$

where θ corresponds to the θ -angle of QCD, L and R denote left- and right-handed quark fields. The lagrangian (13) is obtained from the one-instanton-exchange effective interaction at $\theta = 0$ [33, 34, 55] via a global $U(1)_A$ rotation that removes the gluonic θ -term (1) and encodes all the information about θ into the quark sector. The interaction (13) has already been used in order to study the coupling of the QCD-axion to quarks in a color-superconductive phase [35, 36, 56] and, with suitable modifications, also in the framework of chiral symmetry breaking [2, 57–64], including applications to the study of domain walls [65–69]. For the three-flavor model that we mostly consider in our study, the interaction (13) has to be understood as an effective interaction term in the limit of small quark masses: in this limit, the original six-fermion term becomes effectively a four-quark

interaction [70]. We make this explicit in the definition of the coupling ζ , see below.

The coupling in the interaction (13) is unknown, unless one considers very large values of μ where perturbative calculations are meaningful. In this asymptotic limit, assuming a diagonal quark mass matrix $\mathcal{M} = \text{diag}(M_u, M_d, M_s)$ and putting $M_u = M_d = M_s \equiv M$, for the three-flavor model we would have [55, 70–75]

$$\zeta = M \int d\rho n_0(\rho) \frac{2N_c - 1}{4(N_c^2 - 1)(2N_c)} 2(2\pi\rho)^4 \rho^3. \quad (14)$$

Here n_0 denotes the instanton density,

$$n_0(\rho) = C_N \left(\frac{8\pi^2}{g^2} \right)^{(2N_c)} \rho^{-5} \exp\left(-\frac{8\pi^2}{g^2}\right) e^{-N_f \mu^2 \rho^2}, \quad (15)$$

where ρ is the instanton size. Moreover, N_f is the number of quark flavors, g the QCD coupling (that we assume as independent of the instanton size), N_c is the number of colors and C_{N_c} is a coefficient given by

$$C_{N_c} = 0.466 e^{-1.679 N_c} \frac{1.34^{N_f}}{(N_c - 1)!(N_c - 2)!}. \quad (16)$$

Using a constant g and $N_f = N_c = 3$ we get

$$\zeta = 6.106 \times 10^9 \times \left(\frac{1}{g} \right)^{10} e^{-\frac{8\pi^2}{g^2}} \frac{1}{g^2 \mu^2} \frac{M}{\mu}. \quad (17)$$

Given the uncertainties on the values of g and M at finite μ , we treat ζ as a parameter in our model, and for the sake of simplicity we assume that its dependence on μ , M and g is the one given by Eq. (17). Hence, for a given value of μ we let g and M vary, and fix ζ via Eq. (17). If mass degeneracy is broken then instead of M one should use $\text{Tr}\mathcal{M}/3$ in Eq. (14).

In the CFL phase, the $SU(3)_c$ color symmetry is completely broken, and so is the chiral $SU(3)_A \otimes SU(3)_V$ flavor symmetry with a left $SU(3)_{c+V}$ that combines color and flavor. The ansatz for the quark-quark condensate in the phase is [13]

$$\langle \psi_{\alpha i}^{LT} C \psi_{\beta j}^L \rangle = -\langle \psi_{\alpha i}^{RT} C \psi_{\beta j}^R \rangle \propto \frac{\Delta}{2} \epsilon_{\alpha\beta I} \epsilon_{ij I}. \quad (18)$$

Here, α, β are color indices, i, j are flavor indices, $C = i\sigma_2$, and a sum over $I = 1, 2, 3$ is understood. Δ is the color-superconductive gap parameter, that sets the scale for the gap in the spectrum of the quark quasi-particles. It is useful to introduce the CFL color-flavor basis

$$\psi_{+, \alpha, i} = \sum_{A=1}^9 \frac{\lambda_{A\alpha, i}}{\sqrt{2}} \psi_{+, A}, \quad (19)$$

where λ_A with $A = 1, \dots, 8$ denote the set of Gell-Mann matrices, normalized as $\text{Tr}(\lambda_A \lambda_B) = 2\delta_{AB}$, and $\lambda_9 = \lambda_0 = \sqrt{\frac{2}{3}}\mathbb{I}$. In this basis, the gap matrix reads [16]

$$\Delta_{AB} = \Delta \text{Tr}(\epsilon_I T_A^T \epsilon_I T_B) = \Delta_A \delta_{AB}, \quad (20)$$

with

$$\Delta_A = \begin{cases} \Delta, & A = 1 \cdots 8, \\ -2\Delta, & A = 9, \end{cases} \quad (21)$$

where the first 8 modes are degenerate in an octet and the ninth corresponds to a singlet. This split of the quark spectrum in the CFL phase remains also in case an additional color-sextet contribution is included, see [13, 14, 18, 22, 76]; for the sake of simplicity, we neglect the condensation in the color-sextet channel since its contribution is generally much smaller than that of the anti-triplet interaction [77].

We introduce the Nambu-Gorkov spinor basis as

$$\chi_A = \begin{pmatrix} \psi_{+,A} \\ C\psi_{-,A}^* \end{pmatrix}, \quad (22)$$

with $C = i\sigma_2$. In this basis, the quark-gluon vertex in Eq. (11) can be expressed as:

$$\Gamma_\mu^{aAB} = ig \begin{pmatrix} V_\mu h_{AaB} & 0 \\ 0 & -\tilde{V} h_{AaB}^* \end{pmatrix}, \quad (23)$$

with

$$h_{AaB} = \text{Tr} [T_A T_a T_B], \quad (24)$$

$A, B = 1, \dots, 9$, $a = 1, \dots, 8$ and $T_A = \lambda_A/\sqrt{2}$. The quark-quark interaction mediated by the exchange of one gluon, with vertices (23), is dubbed the one-gluon-exchange (OGE).

In the CFL basis, \mathcal{L}_4 in Eq. (13) reads

$$\mathcal{L}_4 = \zeta \Gamma_{ABCD} \left[(\psi_{LA}^T C \psi_{LB}) (\psi_{RC}^\dagger C \psi_{RD}^*) e^{i\theta} + (\psi_{RA}^T C \psi_{RB}) (\psi_{LC}^\dagger C \psi_{LD}^*) e^{-i\theta} \right], \quad (25)$$

with

$$\Gamma_{ABCD} = \Gamma_{AB} \Gamma_{CD}, \quad \Gamma_{AB} = \text{Tr} (\varepsilon_I T_A^T \varepsilon_I T_B). \quad (26)$$

$\Gamma_{AB} = \Gamma_A \delta_{AB}$ has the same color-flavor structure of the gap matrix, see Eqs. (20) and (21), that is

$$\Gamma_A = \begin{cases} 1, & A = 1 \cdots 8, \\ -2, & A = 9. \end{cases} \quad (27)$$

B. Ansatz on the full quark propagator

In order to define an HDET-2PI effective potential for the CFL phase, we need an ansatz on the full quark propagator, S ; this is a matrix in color-flavor and Nambu-Gorkov spaces. Similarly to previous works, we adopt the following form for S^{-1} for left- and right-handed fields:

$$S_{AB}^{-1}(\ell) = \begin{pmatrix} V \cdot \ell & \Delta_A(\ell) \\ \Delta_A(\ell) & \tilde{V} \cdot \ell \end{pmatrix} \delta_{AB}. \quad (28)$$

Analogously, the inverse free propagator is

$$S_{0,AB}^{-1}(\ell) = \begin{pmatrix} V \cdot \ell & 0 \\ 0 & \tilde{V} \cdot \ell \end{pmatrix} \delta_{AB}. \quad (29)$$

The inversion of Eq. (28) is trivial and leads to

$$S_{AB} = S_A \delta_{AB}, \quad (30)$$

with

$$S_A(\ell) = \frac{1}{V \cdot \ell \tilde{V} \cdot \ell - \Delta_A^2(\ell) + i\varepsilon} \begin{pmatrix} \tilde{V} \cdot \ell & -\Delta_A(\ell) \\ -\Delta_A(\ell) & V \cdot \ell \end{pmatrix}. \quad (31)$$

We will use the ansatz (31) for both left- and right-handed fields in this work.

The off-diagonal component of the inverse quark propagator, $\Delta_A(\ell)$, will be computed by solving the self-consistent gap equation in the 2PI formalism, see Sections III and IV. The interactions that contribute to Δ in our work are the OGE and the OIE interactions. As a final comment, we remark that in this work we consider the static limit, and consider homogeneous and isotropic condensates only, therefore the quark self-energy depends only on ℓ_{\parallel} .

C. 2PI Effective Potential

The Cornwall-Jackiw-Tomboulis (CJT) formalism [27] is a widely used tool in quantum field theory, particularly in contexts where non-perturbative effects and self-consistent treatment of quantum fluctuations play a critical role, such

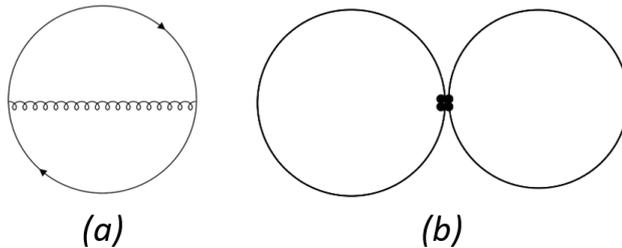


FIG. 1. Two-loop diagrams contributing to V_2 in the CJT potential in Eq. (34). Diagrams (a) and (b) correspond to the OGE and the OIE contact term respectively.

as dynamical symmetry breaking [78–81], out-of-equilibrium dynamics [79, 82, 83], critical and strongly correlated systems [83–85] and stochastic processes [86]. Within this formalism, the concept of the 1PI-effective action [87, 88], which depends on the expectation value of the quantum fields, is improved considering a 2PI-effective action, depending both on the 1-point functions (the field expectation values) and the 2-point functions, the propagators.

Hence, the CJT-effective potential that we use can be expressed as

$$V(S) = -i \int \frac{d^4 p}{(2\pi)^4} \text{Tr} [\ln S_0^{-1}(p)S(p) - S_0^{-1}(p)S(p) + I] + \frac{i}{2} \int \frac{d^4 p}{(2\pi)^4} \text{Tr} [\ln D_0^{-1}(p)D(p) - D_0^{-1}(p)D(p) + I] + V_2(S), \quad (32)$$

where S and D corresponds to the full quark and gluon propagators, respectively, while S_0 and D_0 correspond to the bare ones. $V_2(S)$ corresponds to the sum of all the 2PI vacuum diagrams which are produced by the interaction vertices of the theory, and include the coupling of the quarks to the gluons via the one-gluon-exchange and the one-instanton-exchange. In this work, gluons are dynamical particles, since they have a propagator; however, we do not compute the gluon propagator self-consistently via a DSE coupled to the one for the quark propagator: instead, we use the results obtained non-perturbatively from a different approach [26] that we describe in more detail in the next section. Therefore, the second addendum in the r.h.s. of Eq. (32) is merely a constant and we neglect it in the calculation of the effective potential, and does not contribute to the DSE of the quark propagator. Hence, the CJT potential we consider is

$$V(S) = -i \int \frac{d^4 p}{(2\pi)^4} \text{Tr} [\ln S_0^{-1}(p)S(p) - S_0^{-1}(p)S(p) + I] + V_2(S). \quad (33)$$

Taking into account OGE and OIE terms, we can write V_2 as

$$V_2 = V_2^{\text{OGE}} + V_2^{\text{OIE}}, \quad (34)$$

where

$$V_2^{\text{OGE}} = \text{Tr}[\Gamma S \Gamma D S], \quad (35)$$

and

$$V_2^{\text{OIE}} = \text{Tr}[S \Gamma^t S]. \quad (36)$$

Here, Γ and Γ^t denote the bare vertices of the OGE and OIE interactions respectively. Using the CFL basis (19) we can write the contributions to V_2 as

$$V_2^{\text{OGE}} = \frac{1}{2} \int \frac{d^4 p}{(2\pi)^4} \frac{d^4 k}{(2\pi)^4} \text{Tr} [\Gamma_\mu^{aAC} S_{CD}(p) \Gamma_\nu^{bDB} D_{\mu\nu}^{ab}(p-k) S_{AB}(k)] + (L \rightarrow R), \quad (37)$$

and

$$V_2^{\text{OIE}} = \frac{1}{2} \zeta \int \frac{d^4 p}{(2\pi)^4} \frac{d^4 k}{(2\pi)^4} \text{Tr} [S_{AB}(\ell) \Gamma_{ABCD} S_{CD}(k) e^{i\theta}] + h.c. \quad (38)$$

A diagrammatic representation of (34) is shown in Fig. 1, where (a) and (b) respectively denote the contributions from the OGE and the OIE.

D. Improved gluon Propagator

We now describe the gluon propagator we use in our calculations. At $\mu \neq 0$, as a consequence of the breaking

of Lorentz symmetry, the gluon propagator cannot be

expressed in terms of a single scalar function. Instead, it is determined by two functions $D^T(|\mathbf{p}|)$ and $D^L(|\mathbf{p}|)$ which enter the gluon propagator $D_{\mu\nu}^{ab}(\mathbf{p})$ evaluated at $p^0 = 0$ as

$$D_{\mu\nu}^{ab}(\mathbf{p}) = -\delta^{ab} [D^T(|\mathbf{p}|) P_{\mu\nu}^T(p) + D^L(|\mathbf{p}|) P_{\mu\nu}^L(p)] . \quad (39)$$

In the Landau gauge, assuming that the medium has four-velocity $u^\mu = \delta_{\mu 0}^0$, the projectors $P^T(p)$ and $P^L(p)$ take the form

$$P_{\mu\nu}^T(p) = (1 - \delta_{\mu 0})(1 - \delta_{\nu 0}) \left(g_{\mu\nu} + \frac{p_\mu p_\nu}{|\mathbf{p}|^2} \right), \quad (40)$$

$$P_{\mu\nu}^L(p) = t_{\mu\nu}(p) - P_{\mu\nu}^T(p), \quad (41)$$

where $t_{\mu\nu}(p) = g_{\mu\nu} - p_\mu p_\nu / p^2$ is the usual four-dimensionally transverse projector. They satisfy the chain of equalities

$$P^{T/L}(p) \cdot P^{T/L}(p) = P^{T/L}(p), \quad (42)$$

$$P^T(p) \cdot P^L(p) = 0, \quad (43)$$

$$P^{T/L}(p) \cdot t(p) = t(p) \cdot P^{T/L}(p) = P^{T/L}(p), \quad (44)$$

are both orthogonal to the four-vector p , $P^{T/L}(p) \cdot p = 0$, and in the static limit $p^0 = 0$ they further simplify as

$$P_{\mu 0}^T(p) = P_{0\mu}^T(p) = 0, \quad P_{ij}^T(p) = -\delta_{ij} + \frac{p_i p_j}{|\mathbf{p}|^2}, \quad (45)$$

$$P_{00}^L(p) = 1, \quad P_{\mu i}^L(p) = P_{i\mu}^L(p) = 0. \quad (46)$$

Since $P^T(p)$ is orthogonal to the spatial projection $\bar{p} = (0, \mathbf{p})$ of p , $P^T(p) \cdot \bar{p} = 0$, we will refer to the former as the (three-dimensionally) transverse projector, and to $P^L(p)$ as the (three-dimensionally) longitudinal one; accordingly, we will call $D^T(|\mathbf{p}|)$ and $D^L(|\mathbf{p}|)$ the transverse and the longitudinal component of the gluon propagator.

The evaluation of $D^T(|\mathbf{p}|)$ and $D^L(|\mathbf{p}|)$ is essentially a non-perturbative task. Since for $p^0 = 0$ one has $p^2 = -|\mathbf{p}|^2 < 0$, the components of the gluon propagator could in principle be extracted from the lattice data in Euclidean space. However, at non-vanishing chemical potentials, the lattice is plagued by the infamous sign problem, which limits the applicability of unquenched Monte Carlo methods to domains where the quark determinant is positive, such as QCD at finite isospin density or 2-color QCD at finite baryonic density and an even number of quark flavors. Recent calculations carried out in these domains [89–91] suggest that the transverse component of the gluon propagator is only weakly dependent on chemical potential¹, whereas the longitudinal one gets strongly suppressed as chemical potential increases, a behavior which is consistent with a Debye

mass proportional to chemical potential being generated by the medium in the longitudinal sector. As $\mu \rightarrow 0$, SO(4) rotational invariance – the equivalent of Lorentz invariance in Euclidean space – is restored, and the two components collapse to a unique function which remains finite in the deep infrared, signaling that a dynamical mass is generated for the gluons already in the vacuum by a mechanism which is independent of the medium. This phenomenon has been the subject of numerous studies over the last decades [92–100], is hypothesized to be caused by gluonic condensates [101–103] and is nowadays considered an established feature of the gluon propagator.

Results that display the same behavior as the lattice were recently obtained [26] for the full QCD gluon propagator at finite baryonic chemical potential using a perturbative method known as the screened massive expansion. The latter [104–107] consists in a redefinition of the QCD perturbative series carried out in such a way that the (four-dimensionally) transverse gluons propagate as massive already at tree level, while leaving the action of QCD unchanged; the non-perturbative content of the expansion is condensed in a gluon mass parameter m which must be provided as an external input, e.g. by setting the energy units of the propagator itself. In Fig. 2 we show the propagator computed within the screened massive expansion of full QCD at $\mu = 400, 500, 600$ MeV for $N_f = 2 + 1$ quarks with masses equal to the up/down and strange current masses. The free parameters of the expansion were fixed by extracting the mass scale of the optimized propagator at $\mu = 0$ from pure Yang-Mills lattice data like in [26, 106], which yields a gluon mass parameter $m = 656$ MeV. While the screened massive expansion is able to provide expressions for the propagator which, at finite chemical potential, are analytic up to a one-dimensional integral, in what follows it will be useful to parametrize the components of the propagator using the Gribov-Stingl form

$$D^{T/L}(x) = \frac{Z^{T/L}(x^2 + (m_1^{T/L})^2)}{x^4 + 2(m_2^{T/L})^2 x^2 + (m_3^{T/L})^4}, \quad (47)$$

where $Z^{T/L}$, $m_{1,2,3}^{T/L}$ are free parameters, different for each component and dependent on chemical potential. Their values, as obtained by fitting the propagators in Fig. 2, are reported in Tab. I; the resulting fits are essentially indistinguishable from the propagators obtained by a numerical integration. In the DSE we will make use of the static gluon propagator (47) with $x = |\boldsymbol{\ell} - \mathbf{p}|$, namely

$$D^{T/L}(\boldsymbol{\ell} - \mathbf{p}) = \frac{Z^{T/L}(|\boldsymbol{\ell} - \mathbf{p}|^2 + (m_1^{T/L})^2)}{|\boldsymbol{\ell} - \mathbf{p}|^4 + 2(m_2^{T/L})^2 |\boldsymbol{\ell} - \mathbf{p}|^2 + (m_3^{T/L})^4}, \quad (48)$$

where $\boldsymbol{\ell}$ and \mathbf{p} respectively denote the quark loop and the external quark momenta in the DSE, $|\boldsymbol{\ell} - \mathbf{p}| = \sqrt{\ell_{\parallel}^2 - 2\ell_{\parallel} p \cos \theta_v + p^2}$, and θ_v is the angle between $\boldsymbol{\ell}$ and \mathbf{p} , corresponding to the polar angle in the angular inte-

¹ At least for not too large chemical potentials $\mu \lesssim 800$ MeV, corresponding to $a\mu \ll 1$ (with a the lattice spacing), where the lattice simulations are more reliable.

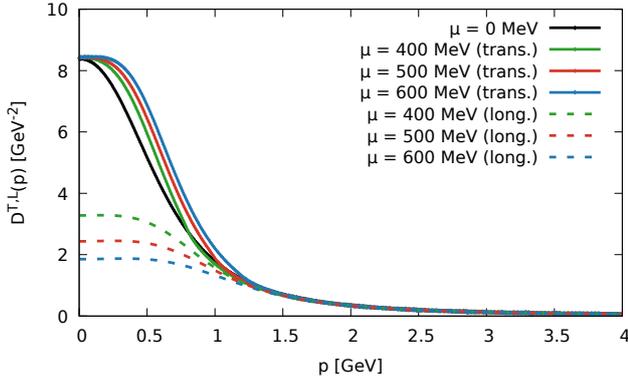


FIG. 2. Transverse and longitudinal components of the gluon propagator $D^{T/L}$ as a function of the 3-momentum $p = |\mathbf{p}|$, for different values of the chemical potential μ .

gration measure (6) since ℓ_{\parallel} and \mathbf{v} are parallel.

III. GAP EQUATION IN THE CFL PHASE

Next, we turn to the gap equation for the CFL phase, written in the formalism of HDET. We define the quark

Taking into account that L and R are degenerate, we get

$$\begin{aligned} \Delta_{AB}(\ell) = & i \frac{4\pi\mu^2}{(2\pi)^4} 2g^2 \sum_v \int d^2\ell V_{\mu} \tilde{V}_{\nu} D_{\mu\nu}(\ell - p) h_{AaC} h_{CaB}^* \frac{\Delta_C(\ell)}{V \cdot \ell \tilde{V} \cdot \ell - \Delta_C^2(\ell) + i0^+} \\ & + i \frac{4\pi\mu^2}{(2\pi)^4} 2\zeta \cos\theta \sum_v \int d\ell^2 \Gamma_{AB} \Gamma_{CD} \frac{\Delta_C(\ell)}{V \cdot \ell \tilde{V} \cdot \ell - \Delta_C^2(\ell) + i0^+} \delta_{CD}. \end{aligned} \quad (52)$$

The overall common coefficient in the two addenda in the right hand side of (52) denotes the HDET integration measure, see Eq. (5), times the 2 that accounts for the $L \rightarrow R$ degeneracy. The $i0^+$ in the denominators of the integrand in the above equation correspond to the standard Feynman prescription to push the negative energy poles to the upper complex ℓ_0 plane.

For the sake of concreteness, we choose the $A = 1$, $B = 1$ element of Σ in Eq. (52). Performing the summation over the internal color-flavor indices, and performing the ℓ_0 integration via the residues we obtain

$$\begin{aligned} \Delta(p) = & -\frac{\mu^2}{6\pi^2} g^2 \sum_v \int d\ell_{\parallel} V_{\mu} \tilde{V}_{\nu} D_{\mu\nu}(\ell - p) \mathcal{W}(\Delta) \\ & + \frac{2\mu^2}{\pi^2} \zeta \cos\theta \sum_v \int d\ell_{\parallel} \Delta(\ell_{\parallel}) (2\mathcal{X}(\Delta) + \mathcal{X}(2\Delta)). \end{aligned} \quad (53)$$

Here we defined

$$\mathcal{X}(\Delta) = \frac{1}{\sqrt{\ell_{\parallel}^2 + \Delta(\ell_{\parallel})^2}}, \quad (54)$$

$$\mathcal{W}(\Delta) = \Delta(\ell_{\parallel}) (\mathcal{X}(\Delta) + \mathcal{X}(2\Delta)). \quad (55)$$

self-energy, Σ , as

$$\Sigma = S^{-1} - S_0^{-1}. \quad (49)$$

The the standard one-loop DSE for the quark propagator can be obtained from the effective potential (33) in the form

$$\Sigma = \Gamma S \Gamma D + \Gamma^t S. \quad (50)$$

In the color-flavor basis of the CFL phase we can write Eq. (50) as

$$\begin{aligned} \Sigma_{AB}(p) = & -i \frac{4\pi\mu^2}{(2\pi)^4} \sum_v \int d^2\ell \Gamma_{\mu}^{aAC} S_{CD}(\ell) \Gamma_{\nu}^{bDB} D_{\mu\nu}^{ab}(\ell - p) \\ & -i \zeta \frac{4\pi\mu^2}{(2\pi)^4} \sum_v \int d^2\ell \Gamma_{ABCD} S_{CD}(\ell) e^{i\theta} \\ & + (L \rightarrow R, \theta \rightarrow -\theta). \end{aligned} \quad (51)$$

We notice that the change $\theta \rightarrow -\theta$ is equivalent to sum up the contributions of the left-handed and right-handed fields in the OIE term. Σ_{AB} in Eq. (51) is still a matrix in the Nambu-Gorkov space; taking the (1, 2) component of Σ in this space space allows us to extract the gap equation.

The $V_{\mu} \tilde{V}_{\nu} D_{\mu\nu}(\ell - p)$ in the equation above can be easily treated by virtue of the straightforward relations

$$P_{\mu\nu}^T(\ell - p) V_{\mu} \tilde{V}_{\nu} = |\mathbf{p}|^2 \frac{1 - \cos^2\theta_v}{\ell_{\parallel}^2 - 2\ell_{\parallel}|\mathbf{p}| \cos\theta_v + |\mathbf{p}|^2} \quad (56)$$

$$P_{\mu\nu}^L(\ell - p) V_{\mu} \tilde{V}_{\nu} = 1. \quad (57)$$

The loop integral involving the OIE term, corresponding to the second term on the right-hand side of Eq. (53), diverges for large momenta. To regulate this divergence, we introduce a cutoff at $\ell_{\parallel} = \Lambda$. The cutoff value is fixed to $\Lambda = 200$ MeV, consistent with previous studies within the HDET framework [15, 16].

Equation (53) represents the gap equation in the form we solve numerically. Due to the use of a non-local interaction kernel, the gap equation takes the form of a non-linear integral equation for the function $\Delta(\ell)$. In the

μ [MeV]	Z^T	m_1^T [MeV]	m_2^T [MeV]	m_3^T [MeV]	Z^L	m_1^L [MeV]	m_2^L [MeV]	m_3^L [MeV]
400	1.06518	1086.16	301.016	621.807	0.994707	1376.83	345.026	870.951
500	0.895304	1400.91	268.164	675.740	0.922562	1576.92	338.641	985.201
600	0.823320	1611.01	220.258	709.165	0.879109	1747.78	351.646	1096.94

TABLE I. Parameters used to fit the gluon propagator with the Gribov-Stingl form (47).

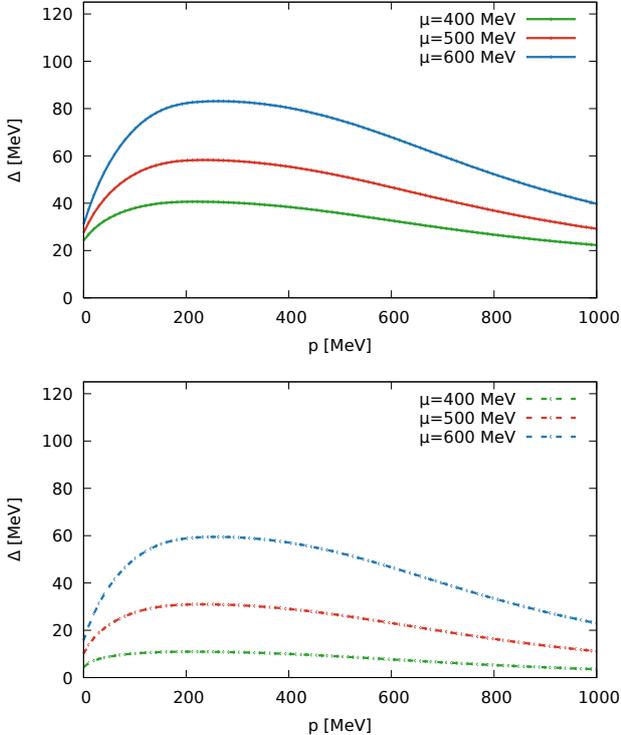


FIG. 3. Solution of the gap equation Δ as a function of the external momentum p in the CFL phase for different values of the of the chemical potential μ at fixed gauge coupling $g = 2.8$ and at $\theta = 0$. Upper panel corresponds to the solution of the full gap equation, while in the lower panel we show the results obtained neglecting the OIE term.

next section, we present some of the numerical solutions of Eq. (53).

IV. SOLUTION OF THE GAP EQUATION FOR THE CFL PHASE

In this section we present our results for the solution of the gap equation in the CFL phase. We used a fixed-coupling scheme, in which we firstly fixed $\alpha_s = g^2/4\pi$ at the scale μ with the one-loop β -function, giving $\alpha_s = 1.007, 0.762, 0.635$ respectively for $\mu = 400, 500, 600$ MeV. Then, we have $g = 3.558, 3.094, 2.826$ for the same values of μ . We then fixed $\Lambda = 200$ MeV in agreement with previous calculations in HDET [16]. With this choice of parameters we get $\Delta(p=0) \sim 20 - 40$ MeV in the range of μ considered here, in agreement with previ-

ous studies [17, 24, 25, 108]. Finally, we use $M = 100$ MeV for ζ in Eq. (14), which is a fair averaged value of the light and strange quarks masses, in agreement with estimates of the constituent quark masses within Nambu-Jona-Lasinio models [18, 19, 109]. The use of an average value of the constituent quark mass is justified by the fact that ζ in Eq. (14) is actually proportional to the trace of the quark mass matrix.

In Fig. 3 we plot the superconductive gap solution of the gap equation (53) versus the external momentum p , for $\mu = 400, 500$ and 600 MeV. In the upper panel of the figure we show the solution of the full gap equation, while in the lower panel we plot the results obtained neglecting the OIE term in the gap equation. Firstly, we notice that overall the contribution of the latter interaction to the gap is substantial. Then, we notice that for a given value of μ , our solution shows a maximum at $p \neq 0$, in qualitative agreement with previous results based on one-gluon-exchange models [25, 108]. The presence of a maximum for $p \neq 0$ is specific to the gluon propagator used in the gap equation. Furthermore, as expected from our calculations and in agreement with results known in the literature [17, 24, 25], the value of the gap increases as the chemical potential is increased.

We denote by Δ_t the solution of the full gap equation (53) in the limit $p \rightarrow \infty$. For large external momentum $p \rightarrow \infty$, the gap equation receives contributions only from the contact OIE term, as the term associated with one-gluon exchange on the right-hand side of the equation vanishes due to the asymptotic behavior of the gluon propagator. From Eq. (53) we get

$$\Delta_t = \frac{2\mu^2}{\pi^2} \zeta \cos \theta \sum_v \int d\ell_{\parallel} \Delta(\ell_{\parallel}) (2\mathcal{X}(\Delta) + \mathcal{X}(2\Delta)), \quad (58)$$

where $\Delta(\ell_{\parallel})$ denotes the solution of the gap equation in the whole momentum range, and \mathcal{X} is defined in Eq. (54). The relation (58) offers an analytical relation between the integrals on the right-hand side of the equation and Δ_t , that we will use to obtain a compact expression of χ in the next section.

It is interesting to analyze the contribution of the OGE and OIE interactions to the CFL gap. This is shown in Fig. 4, where we plot the solution of the full gap equation at $p = 0$ versus the coupling g for $\mu = 400$ MeV (upper panel) and $\mu = 600$ MeV (lower panel). In the two plots, we split the contributions of the OGE and OIE to the gap, which are obtained as the two addenda of the right hand side of Eq. (52) in which we substitute the solution

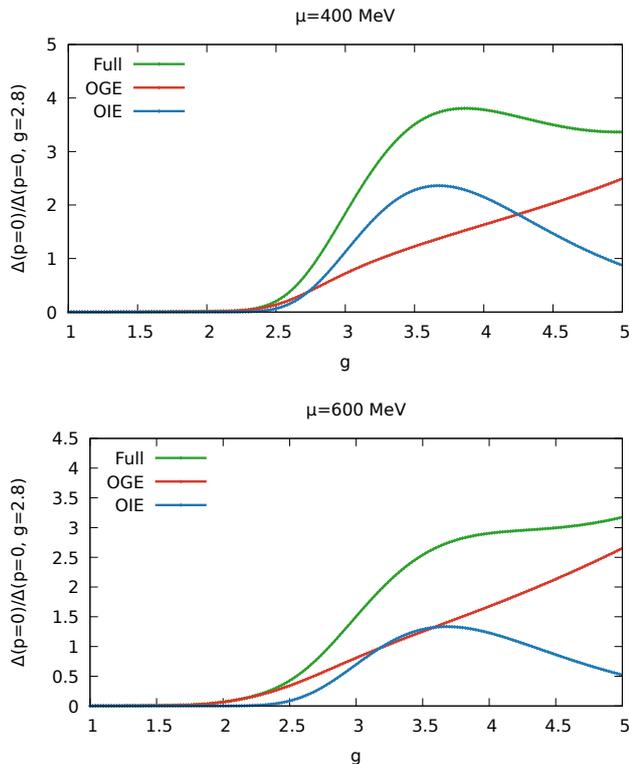


FIG. 4. Solution of the gap equation Δ evaluated at vanishing momentum $p = 0$ versus the OGE coupling, g , at $\theta = 0$, for $\mu = 400$ MeV (upper panel) and $\mu = 600$ MeV (lower panel), in the CFL phase of high-density QCD. For each value of the chemical potential, the curves are normalized to the value of the solution of the gap equation at vanishing momentum $\Delta(p = 0)$ for $g = 2.8$.

of the gap equation. We notice that the relative contribution of the two interactions to the gap is very sensitive of the value of the chemical potential considered, as well as of g . For $g = 2.8$ and $\mu = 600$ MeV, the contribution of the two interactions is similar in magnitude. On the other hand, for $\mu = 600$ MeV and the same value of g , the OIE interaction gives a relatively smaller contribution. These considerations help to extract the dependence of the topological susceptibility on the couplings in Section VII.

V. TOPOLOGICAL SUSCEPTIBILITY IN THE CFL PHASE

The main goal of this study is the computation of the topological susceptibility. Identifying the CJT effective potential, V , with the thermodynamic potential Ω , we obtain an expression for χ starting from V , that is

$$\chi = \left. \frac{d^2 V(\Delta(p; \theta), \theta)}{d\theta^2} \right|_{\theta=0}. \quad (59)$$

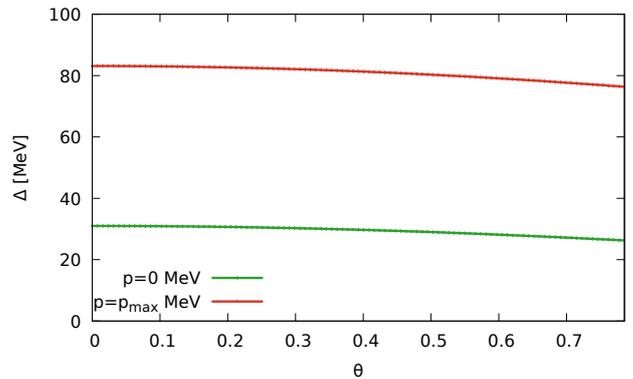


FIG. 5. Solution of the gap equation Δ as a function of θ at fixed momenta for fixed gauge coupling $g = 2.8$ and $\mu = 600$ MeV, in the CFL phase. Δ is evaluated at vanishing momentum and at p_{max} for which $\Delta(p; \theta = 0)$ reaches its maximum (see Fig. 3).

In (59) we denoted by $\Delta(p; \theta)$ the solution of the gap equation, that depends on momentum as well as on θ .

In principle, one should take the total derivative of the thermodynamic potential with respect to θ , hence considering both the explicit and the implicit θ -dependence of V . This was the case for the calculation of the topological susceptibility at $\mu = 0$ [2, 36]. However, our theory remains invariant under the transformation $\theta \rightarrow -\theta$. In contrast to the case of chiral and η -condensates at $\mu = 0$, where both scalar and pseudo-scalar condensates exist for $\theta \neq 0$ —even for small θ —and $\partial\eta/\partial\theta \neq 0$ [36], in superconducting phases, we find only the scalar condensate [35], unless $\theta \geq \pi/2$. As a result, the effective potential is an even function of θ . This implies that every real observable, including the gap Δ , must also be an even function of θ , hence $\partial\Delta/\partial\theta = 0$ at $\theta = 0$. This behavior is confirmed by the solution of the full gap equation at finite θ , see Fig. 5, in which we notice that Δ versus θ is flat for $\theta \rightarrow 0$. Using this property, a straightforward application of the chain rule shows that, when computing χ , we only need to consider the explicit dependence of the effective potential on θ . The only explicit dependence of V on θ appears in V_2^{OIE} in Eq. (38). Therefore, instead of Eq. (59), we use

$$\chi = \left. \frac{\partial^2 V_2^{\text{OIE}}(\Delta(p; \theta), \theta)}{\partial\theta^2} \right|_{\theta=0}. \quad (60)$$

In the HDET formulation, we can write Eq. (38) as

$$V_2^{\text{OIE}} = \frac{1}{2} \frac{4\mu^4}{(2\pi)^6} \zeta \sum_{v, v'} \int d^2\ell d^2k \text{Tr} [\mathcal{R}(\ell, k) e^{i\theta}] + h.c., \quad (61)$$

where

$$\mathcal{R}(\ell, k) = S_{AB}(\ell) \Gamma_{ABCD} S_{CD}(k). \quad (62)$$

In Eq. (61) v and v' denote the Fermi velocities related to the loops in ℓ and k respectively. The result (61) stands

for any color-superconductive phase, because we have not made any assumption on the quark propagator. We now specialize it to the case of the CFL phase. Taking into account Eqs. (26) and (30), with S_A given by Eq. (31), we obtain

$$V_2^{\text{OIE}} = \frac{\mu^4}{(2\pi)^6} \zeta \cos \theta \int d^2 \ell d^2 k \text{Tr} [S_A(\ell) \Gamma_{AA} \Gamma_{CC} S_C(k)], \quad (63)$$

from which we derive

$$\chi = -\frac{\mu^4}{(2\pi)^6} \zeta \int d^2 \ell d^2 k \text{Tr} [S_A(\ell) \Gamma_{AA} \Gamma_{CC} S_C(k)]. \quad (64)$$

A straightforward calculation of the trace and of the integral over ℓ_0 by residues leads at

$$\chi = \frac{\mu^4}{2\pi^4} \zeta \left[2 \int d\ell_{\parallel} \frac{\Delta(\ell_{\parallel}, \theta = 0)}{\sqrt{\ell_{\parallel}^2 + \Delta(\ell_{\parallel}^2, \theta = 0)}} + \int d\ell_{\parallel} \frac{\Delta(\ell_{\parallel}, \theta = 0)}{\sqrt{\ell_{\parallel}^2 + 4\Delta(\ell_{\parallel}^2, \theta = 0)}} \right]^2. \quad (65)$$

We notice that the two addenda in the square bracket in Eq. (65) can be directly related to the solution of the gap equation for $p \rightarrow \infty$ and $\theta = 0$, Δ_t , see Eq. (58). We therefore get

$$\chi = \frac{\Delta_t^2}{2\zeta}. \quad (66)$$

This is one of the main results of this article: it expresses the topological susceptibility of the CFL phase in terms of the gap in the large-momentum limit, and the value of the OIE coupling ζ .

We also notice that the functional dependence of χ on ζ and Δ_t in Eq. (66) stands regardless of the gluon propagator used in the DSE for the quark self-energy: the former can only modify the momentum-dependence of the superconductive gap, and consequently the numerical value of Δ_t , but does not directly affect Eqs. (65) and (58).

In order to give concrete numerical values of χ obtained within our calculation, we quote the result at $\mu = 600$ and $g = 2.8$, that corresponds to the solution of the gap equation $\Delta_t = 11.9$ MeV: we find

$$\chi^{1/4} = 111 \text{ MeV}, \quad \mu = 600 \text{ MeV}. \quad (67)$$

Similarly, for $\mu = 500$ MeV we find $\Delta_t = 12.3$ MeV and

$$\chi^{1/4} = 98 \text{ MeV}, \quad \mu = 500 \text{ MeV}. \quad (68)$$

This number is of the same order of magnitude of χ obtained in [35] for the 2SC phase, which sits in the range 50 – 75 MeV for $\mu = 400$ MeV and $\Delta = 25$ MeV.

In Fig. 6 we plot $\chi^{1/4}$ versus the OGE coupling, g , for several values of μ in the CFL phase. Qualitatively, χ

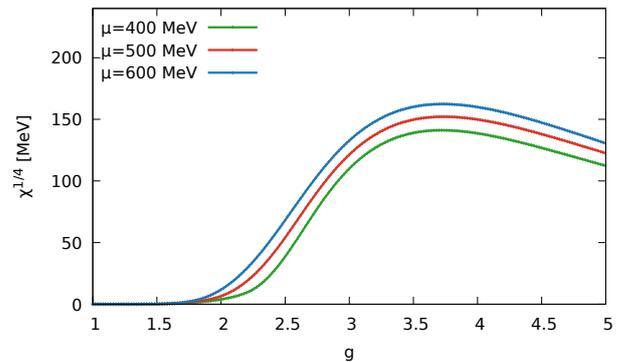


FIG. 6. $\chi^{1/4}$ as a function of the OGE coupling, g , for several values of μ , in the CFL phase.

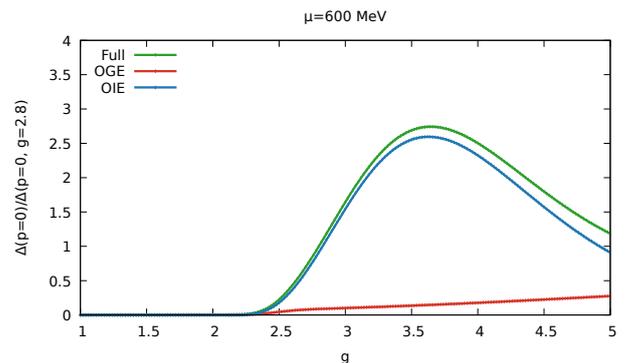


FIG. 7. Solution of the gap equation Δ evaluated at vanishing momentum $p = 0$ versus the OGE coupling, g , at $\theta = 0$, for $\mu = 600$ MeV in the 2SC phase of high-density QCD. The curves are normalized to the value of the solution of the gap equation at vanishing momentum $\Delta(p = 0)$ for $g = 2.8$.

increases with g , due to the increase of Δ_t . We notice a strong dependence of χ on g , which we extract below in two limiting cases. One of the messages encoded in the figure is that that an uncertainty on g in the CFL phase results in a substantial uncertainty on ζ and χ .

VI. TOPOLOGICAL SUSCEPTIBILITY IN THE 2SC PHASE

Here we briefly extend our previous discussion to the 2SC phase. In this phase, the quark-quark condensate is given by [17, 25]

$$\langle \psi_{\alpha i}^{LT} C \psi_{\beta j}^L \rangle = -\langle \psi_{\alpha i}^{RT} C \psi_{\beta j}^R \rangle \propto \frac{\Delta}{2} \epsilon_{\alpha\beta 3} \epsilon_{ij 3}, \quad (69)$$

instead of Eq. (69). Hence, the condensate in the 2SC phase involves u and d quarks only, with colors red and green. The $U(1)_A$ -breaking term has the same form as

in Eq. (13), with

$$\zeta = \int d\rho n_0(\rho) \left(\frac{4}{3\pi^2 \rho^3} \right)^2. \quad (70)$$

Analogously to the CFL case, the first step is to solve the gap equation. It is possible to formulate the quark propagator and the whole DSE using a change in the color-flavor basis which is completely analogous to Eq. (19) (for more details one can refer to [15]). Following straightforward steps, analogous to the ones that leads to Eq. (53), one can easily obtain the gap equation for the 2SC phase

$$\begin{aligned} \Delta(p) = & -\frac{\mu^2}{3(2\pi)^2} g^2 \sum_v \int d\ell_{\parallel} V_{\mu} \tilde{V}_{\nu} D_{\mu\nu}(\ell - p) \frac{\Delta(\ell_{\parallel})}{\sqrt{\ell_{\parallel}^2 + \Delta^2(\ell_{\parallel})}} \\ & + \frac{2\mu^2}{\pi^2} \zeta \cos \theta \sum_v \int d\ell_{\parallel} \frac{\Delta(\ell_{\parallel})}{\sqrt{\ell_{\parallel}^2 + \Delta(\ell_{\parallel})^2}}. \end{aligned} \quad (71)$$

As for the CFL case, we can then define the contribution to the gap equation which arises from the OIE vertex considering the $p \rightarrow \infty$ limit

$$\Delta_t = \frac{\mu^2}{\pi^2} \zeta \cos \theta \int d\ell_{\parallel} \frac{\Delta(\ell_{\parallel})}{\sqrt{\ell_{\parallel}^2 + \Delta(\ell_{\parallel})^2}}. \quad (72)$$

Armed with the solution of the gap equation, one can proceed analogously to the steps that led to (65) and obtain the expression for the topological susceptibility in the 2SC phase, that is

$$\chi = \frac{\mu^4}{2\pi^4} \zeta \left(\int d\ell_{\parallel} \frac{\Delta(\ell_{\parallel}, \theta = 0)}{\sqrt{\ell_{\parallel}^2 + \Delta^2(\ell_{\parallel}, \theta = 0)}} \right)^2. \quad (73)$$

We notice that, combining Eq. (72) and Eq. (73) we obtain

$$\chi = \frac{\Delta_t^2}{2\zeta}. \quad (74)$$

that formally coincides with Eq. (66). We hence find that the topological susceptibility in the 2SC and the CFL phases depends in the same fashion on ζ and Δ_t : the numerical differences between the values of χ in the two phases is encoded Δ_t and ζ .

As an indication, for $g = 2.8$ and $\mu = 600$ MeV, which are the same values we used for the estimate (67) of χ in the CFL phase, in the 2SC phase we find $\Delta(p = 0) = 208.8$ MeV, $\Delta_t = 190.5$ MeV and

$$\chi^{1/4} = 182 \text{ MeV}, \quad \mu = 600 \text{ MeV}. \quad (75)$$

Similarly, for $\mu = 500$ MeV we find $\Delta(p = 0) = 205.1$ MeV, $\Delta_t = 188.5$ MeV and

$$\chi^{1/4} = 165 \text{ MeV}, \quad \mu = 500 \text{ MeV}. \quad (76)$$

The result (74) is analogous to the one obtained in [35], in which χ was computed within an effective model with a contact interaction both in the one-gluon-exchange and in the OIE channels for the 2SC phase, namely

$$\chi = \frac{\Delta^2}{2G_D} \xi \frac{2 - \xi}{2 + \xi}. \quad (77)$$

Here, Δ stands for the solution of the gap equation, that takes contribution both from the one-gluon-exchange and the OIE channels (both of them are momentum-independent in [35], therefore the one-gluon-exchange contribution does not vanish as it happens within our model for $p \rightarrow \infty$). Moreover, G_D denotes the strength of the coupling in the one-gluon-exchange channel, and ξ corresponds to the ratio between the couplings in the OIE and OGE channels, that was treated as a free parameter. One of the improvements that we bring in the present work for the calculation of χ , in comparison to [35], are that we adopt a calculation scheme based on a DSE for the quark propagator that is more easily related to full QCD than effective models: indeed, our results depend solely on the QCD coupling, g , on the strength of the OIE term, which is computed from the theory of QCD instantons at large μ and is fully specified as soon as g and μ are known. Moreover, we allow for a momentum-dependence of the superconductive gap, which is the natural consequence of the use of an improved gluon propagator in the kernel of the gap equation.

VII. TOPOLOGICAL SUSCEPTIBILITY IN LIMITING CASES

As a theoretical exercise, we analyze the dependence of χ on ζ in two limiting cases, assuming, for illustrative purposes, that the gap equation is dominated either by the OGE or the OIE. While such a dominance is not observed in our results, this analysis provides insight into the potential behavior of the system under extreme assumptions.

To begin with, we analyze χ in the CFL phase, considering the case in which the OGE dominates the CFL gap equation. In this regime, on the right-hand side of Eq. (58), we can use the solution of Eq. (53) for $\zeta = 0$, leading to $\Delta_t \propto \zeta$ in the weak coupling limit. This implies

$$\chi \approx \zeta \frac{\mu^4}{2\pi^4} \mathcal{Y}, \quad (78)$$

where we put

$$\begin{aligned} \mathcal{Y} = & \left[2 \int d\ell_{\parallel} \frac{\Delta(\ell_{\parallel}, \theta = 0)_{\text{oge}}}{\sqrt{\ell_{\parallel}^2 + \Delta(\ell_{\parallel}^2, \theta = 0)_{\text{oge}}}} + \right. \\ & \left. \int d\ell_{\parallel} \frac{\Delta^2(\ell_{\parallel}, \theta = 0)_{\text{oge}}}{\sqrt{\ell_{\parallel}^2 + 4\Delta^2(\ell_{\parallel}^2, \theta = 0)_{\text{oge}}}} \right]^2, \end{aligned} \quad (79)$$

and $\Delta(\ell_{\parallel}^2, \theta = 0)_{\text{oge}}$ corresponds to the solution of the gap equation for $\zeta = 0$.

Next, we turn to the case in which the OIE contribution dominates the gap equation. In the CFL phase this In this case, we can approximate $\Delta(\ell_{\parallel}) \approx \Delta_t$ for any ℓ_{\parallel} . In this limit, Eq. (58) for $\theta = 0$ turns to

$$1 = \frac{2\mu^2}{\pi^2} \zeta \sum_v \int d\ell_{\parallel} \left(\frac{2}{\sqrt{\ell_{\parallel}^2 + \Delta_t^2}} + \frac{1}{\sqrt{\ell_{\parallel}^2 + 4\Delta_t^2}} \right) \quad (80)$$

which looks like the standard BCS gap equation at $T = 0$ for a contact four-fermion interaction. The integral on the right hand side of Eq. (80) can be computed as in the BCS theory, namely restricting the integration domain to a shell around the Fermi surface (corresponding to $\ell_{\parallel} = 0$ in HDET) with width δ . Assuming $\delta \gg \Delta_t$ we get

$$\Delta_t = \delta \exp\left(-\frac{\pi^2}{6\zeta\mu^2}\right), \quad (81)$$

that is, Δ_t increases with ζ . As a consequence,

$$\chi \approx \frac{\delta^2}{2\zeta} \exp\left(-\frac{\pi^2}{3\zeta\mu^2}\right). \quad (82)$$

For the 2SC phase we can repeat the same arguments that lead at Eqs. (78) and (82). In the limiting case in which the OGE is more important, χ is given by Eq. (78) with

$$\mathcal{Y} = \left[\int d\ell_{\parallel} \frac{\Delta(\ell_{\parallel}, \theta = 0)_{\text{oge}}}{\sqrt{\ell_{\parallel}^2 + \Delta(\ell_{\parallel}, \theta = 0)_{\text{oge}}^2}} \right]^2. \quad (83)$$

In the limit in which the OIE dominates the gap, instead of Eq. (80) we get from Eq. (72)

$$1 = \frac{\mu^2}{\pi^2} \zeta \sum_v \int d\ell_{\parallel} \frac{1}{\sqrt{\ell_{\parallel}^2 + \Delta_t^2}}, \quad (84)$$

which gives

$$\Delta_t = 2\delta \exp\left(-\frac{\pi^2}{\zeta\mu^2}\right), \quad (85)$$

instead of Eq. (81). Consequently,

$$\chi \approx \frac{2\delta^2}{\zeta} \exp\left(-\frac{2\pi^2}{\zeta\mu^2}\right). \quad (86)$$

instead of Eq. (82).

VIII. COMMENTS ON THE AXION MASS

The calculation of the effective potential in Eq. (33) allows us to directly access the low-energy properties of the QCD axion. In particular, the axion mass, m_a , is

related to the topological susceptibility χ via the relation $\chi = m_a^2 f_a^2$, where f_a is the axion decay constant. From Eqs. (66) and (74) we obtain

$$m_a^2 = \frac{\Delta_t^2}{2\zeta f_a^2} \quad (87)$$

for the CFL and the 2SC phases. Since f_a is not a QCD scale, it is unlikely to be modified during the transition from nuclear matter to quark matter. Moreover, it cannot be computed within our framework. However, constraints on this quantity are available from various astrophysical and cosmological observations (see [110–112] for astrophysical bounds).

Within our formalism, Eq. (87) is exact and allows us to express the axion mass in the CFL and 2SC phases of QCD solely in terms of the superconducting gap and the OIE coupling. The details of the QCD interaction leading to color superconductivity are encapsulated in the value of Δ_t and do not alter the analytical dependence of m_a on the gap.

Our result, Eq. (87), can be compared with previous works, such as [35], where it was found that

$$m_a^2 = \frac{\Delta^2}{2G_D f_a^2} \xi \frac{2 - \xi}{2 + \xi}. \quad (88)$$

The improvement provided by Eq. (87) over Eq. (88) is that m_a in Eq. (87) is expressed purely in terms of QCD parameters, rather than in terms of parameters from effective models. Apart from the relation with the OIE coupling, which is computed at large μ and expressed solely in terms of g , all details of the gap equation kernel are embedded in Δ_t .

We find that χ in the superconducting phases is of the same order as in the vacuum. Therefore, one of the consequences of our work is that the axion mass in these phases can be as large as at $\mu = 0$, provided that phase transitions to color-superconducting phases occur in dense matter. This result is in agreement with [35, 36] but differs from that in [1], where color superconductivity was not included, and the only phase transition considered was that to normal quark matter. Thus, if the transition to the color-superconducting phase at large μ is preceded, at lower μ , by a normal quark matter phase, then we expect a decrease in m_a in the latter phase, followed by an increase in the former. On the other hand, if the transition from nuclear matter to quark matter occurs without an intermediate- μ phase, then m_a might not undergo a significant change from its vacuum value.

It is certainly interesting to extend these considerations to other low-energy properties of the QCD axion, *in primis*, the axion self-coupling. This investigation will be pursued in future works.

IX. CONCLUSIONS AND OUTLOOK

We computed the topological susceptibility, χ , in the color-superconductive phases of Quantum Chromody-

namics (QCD) at zero temperature and large quark chemical potential, μ . We focused on the Color-Flavor-Locking (CFL) and the 2-Color-Superconductor (2SC) phases. For the CFL, we assume the quarks have an average constituent mass M , whose value is borrowed from the results of NJL-like models at finite μ , while for the 2SC phase we assume massless u and d quarks.

Our calculation scheme combines for the first time the High Density Effective Theory (HDET) at finite θ to the 2-particle irreducible formalism, that we use to derive the Dyson-Schwinger equation (DSE) for the quark propagator in the rainbow approximation (bare vertices) and fixed-coupling. In the kernel of the DSE we use both an improved gluon propagator and a local vertex, that respectively describe the contributions of the one-gluon-exchange (OGE) and of the one-instanton-exchange (OIE) interactions to the superconductive gap. For the sake of simplicity, we work in the static limit of the gluon propagator, which implies that the gap function, Δ , does not depend on energy. The gap equation in this formalism leads to a non-linear integral equation, that we solve numerically.

Within our calculation scheme, for the CFL phase there are only three free parameters in the quark sector, that are the OGE coupling, g , the average quark mass, M , and the cutoff, Λ , that regulates the divergence of the OIE loop in the gap equation. In the 2SC phase, the quark masses are assumed to vanish, so we are left with g and Λ as free parameters. We fixed g at the scale μ via the one-loop QCD β -function. The value of Λ has been fixed in agreement with previous calculations in HDET [16]. The strength of the OIE coupling, ζ , has been fixed by the perturbative results at finite μ . The gluon propagator was instead borrowed from [26], and entails non-perturbative mass scales arising both from vacuum and from matter effects. We regularized the theory via the introduction of the cutoff Λ .

We derived an analytical result for the topological susceptibility in the CFL and 2SC phases, see Eq. (66), which stands regardless of the specific form of the gluon propagator used in the OGE contribution to the gap equation. In fact, we were able to express χ as a function of ζ and Δ_t , namely the solution of the gap equation in the large- p limit. Our calculations give values of χ that are of the same order of those in the vacuum both for the CFL and for the 2SC phases. This result is in some agreement with previous calculations based on effective models with a contact interaction [35, 36], where however there is some additional uncertainty on the final prediction for χ due to the treatment of the ratio of the couplings in the OGE and OIE as a free parameter. We also derived two limiting behaviors of χ versus ζ , for the cases in which

the gap equation is dominated either by the OGE or by the OIE kernels, highlighting a linear increase of χ in the former case, and a BCS-like dependence of χ in ζ in the latter case, see Eqs. (78) and (82) respectively.

Finally, we related our findings for χ to the QCD-axion mass, m_a . In fact, we propose Eq. (87) as a relation between m_a , the superconductive gap and ζ , which stands both in the CFL and the 2SC phases. From the fact that the values of χ in the superconductive phases are in the same ballpark of those in the vacuum, suggests that m_a in superdense QCD phases might be as large as that in the vacuum. This is different from the behavior of m_a found in [1] where color superconductivity was not considered, and m_a was found to be quite smaller than its vacuum value. Hence, if a phase transition happens directly from nuclear matter to superconductive quark matter, as strong-coupling scenarios seem to suggest [19, 109] then m_a at large μ might not be very different from its value in the vacuum, see also [36]. Moreover, since the topological susceptibility can be directly related to the surface tension of the axion walls [1, 36], our results suggest that the surface tension of these walls in superdense QCD phases might be as large as that in the vacuum.

Admittedly, our approach to the DSE is oversimplified in comparison with a full QCD approach. Indeed, we employ an HDET version of the effective potential and of the gap equation of dense QCD, consider the static approximation for the quark and the gluon propagator, ignore the backreaction of color superconductivity to the gluon propagator (although the latter contains screening effects, computed non-perturbatively in [26]), and adopt the rainbow approximation for the quark-gluon vertex. Nevertheless, ours is a first step to the application of Dyson-Schwinger equations in dense QCD to the calculation of the topological susceptibility, and paves the way for more refined calculations that remove the simplifications we have done. More work on this subject is ongoing and we plan to report on it in future works.

Acknowledgments

M. R. acknowledges Bruno Barbieri, Lautaro Martinez and John Petrucci for inspiration. M. R. acknowledges discussions with Ana G. Grunfeld and David E. Alvarez Castillo. This work has been partly funded by PIACERI “Linea di intervento 1” (M@uRHIC) of the University of Catania, and the European Union – Next Generation EU through the research grants number P2022Z4P4B “SOPHYA - Sustainable Optimised PHYSICS Algorithms: fundamental physics to build an advanced society” and 2022SM5YAS, under the program PRIN 2022 PNRR of the Italian Ministero dell’Università e Ricerca (MUR).

[1] B. Zhang, D. E. A. Castillo, A. G. Grunfeld, and M. Ruggieri, Exploring the axion potential and axion

walls in dense quark matter, Phys. Rev. D **108**, 054010

- (2023), arXiv:2304.10240 [hep-ph].
- [2] Z. Y. Lu and M. Ruggieri, Effect of the chiral phase transition on axion mass and self-coupling, *Phys. Rev. D* **100**, 014013 (2019), arXiv:1811.05102 [hep-ph].
- [3] R. Gatto and M. Ruggieri, Hot Quark Matter with an Axial Chemical Potential, *Phys. Rev. D* **85**, 054013 (2012), arXiv:1110.4904 [hep-ph].
- [4] M. Ruggieri, M. N. Chernodub, and Z.-Y. Lu, Topological susceptibility, divergent chiral density and phase diagram of chirally imbalanced QCD medium at finite temperature, *Phys. Rev. D* **102**, 014031 (2020), arXiv:2004.09393 [hep-ph].
- [5] S. A. et al. [JLQCD], Topological susceptibility in 2+1-flavor qcd with chiral fermions, *EPJ Web Conf.* **175**, 04008 (2018), arXiv:1712.05541 [hep-lat].
- [6] Y. Y. M. et al. [TWQCD], Topological susceptibility to the one-loop order in chiral perturbation theory, *Phys. Rev. D* **80**, 034502 (2009), arXiv:0903.2146 [hep-lat].
- [7] G. Grilli di Cortona, E. Hardy, J. Pardo Vega, and G. Villadoro, The qcd axion, precisely, *JHEP* **01**, 034, arXiv:1511.02867 [hep-ph].
- [8] G. Landini and E. Meggiolaro, Study of the interactions of the axion with mesons and photons using a chiral effective Lagrangian model, *Eur. Phys. J. C* **80**, 302 (2020), arXiv:1906.03104 [hep-ph].
- [9] S. Bottaro and E. Meggiolaro, QCD axion and topological susceptibility in chiral effective Lagrangian models at finite temperature, *Phys. Rev. D* **102**, 014048 (2020), arXiv:2004.11901 [hep-ph].
- [10] S. Borsanyi, Z. Fodor, J. Guenther, K. H. Kampert, S. D. Katz, T. Kawanai, T. G. Kovacs, S. W. Mages, A. Pasztor, and F. Pittler, Calculation of the axion mass based on high-temperature lattice quantum chromodynamics, *Nature* **539**, 69 (2016), arXiv:1606.07494 [hep-lat].
- [11] C. Bonati, M. D’Elia, M. Mariti, G. Martinelli, M. Mesiti, F. Negro, F. Sanfilippo, and G. Villadoro, Axion phenomenology and θ -dependence from $n_f = 2 + 1$ lattice qcd, *JHEP* **03**, 155, arXiv:1512.06746 [hep-lat].
- [12] V. Bernard, S. Descotes-Genon, and G. Toucas, Topological susceptibility on the lattice and the three-flavour quark condensate, *JHEP* **06**, 051, arXiv:1203.0508 [hep-ph].
- [13] M. G. Alford, K. Rajagopal, and F. Wilczek, Color flavor locking and chiral symmetry breaking in high density QCD, *Nucl. Phys. B* **537**, 443 (1999), arXiv:hep-ph/9804403.
- [14] K. Rajagopal and F. Wilczek, The Condensed matter physics of QCD, in *At the frontier of particle physics. Handbook of QCD. Vol. 1-3*, edited by M. Shifman and B. Ioffe (2000) pp. 2061–2151, arXiv:hep-ph/0011333.
- [15] G. Nardulli, Effective theory for QCD in the LOFF phase, *eConf* **C010815**, 104 (2002), arXiv:hep-ph/0111178.
- [16] G. Nardulli, Effective description of qcd at very high densities, *Riv. Nuovo Cim.* **25N3**, 1 (2002), arXiv:hep-ph/0202037 [hep-ph].
- [17] T. Schäfer and F. Wilczek, Superconductivity from perturbative one gluon exchange in high density quark matter, *Phys. Rev. D* **60**, 114033 (1999), arXiv:hep-ph/9906512.
- [18] M. Buballa, Njl model analysis of quark matter at large density, *Phys. Rept.* **407**, 205 (2005), arXiv:hep-ph/0402234 [hep-ph].
- [19] D. Blaschke, S. Fredriksson, H. Grigorian, A. M. Oztas, and F. Sandin, The phase diagram of three-flavor quark matter under compact star constraints, *Phys. Rev. D* **72**, 065020 (2005), arXiv:astro-ph/0504361 [astro-ph].
- [20] M. G. Alford, A. Schmitt, K. Rajagopal, and T. Schäfer, Color superconductivity in dense quark matter, *Rev. Mod. Phys.* **80**, 1455 (2008), arXiv:0709.4635 [hep-ph].
- [21] I. A. Shovkovy, Two lectures on color superconductivity, *Found. Phys.* **35**, 1309 (2005), arXiv:nucl-th/0410091 [nucl-th].
- [22] I. A. Shovkovy and L. C. R. Wijewardhana, On gap equations and color flavor locking in cold dense QCD with three massless flavors, *Phys. Lett. B* **470**, 189 (1999), arXiv:hep-ph/9910225.
- [23] R. Gatto and M. Ruggieri, On the ground state of gapless two flavor color superconductors, *Phys. Rev. D* **75**, 114004 (2007), arXiv:hep-ph/0703276.
- [24] D. T. Son, Superconductivity by long range color magnetic interaction in high density quark matter, *Phys. Rev. D* **59**, 094019 (1999), arXiv:hep-ph/9812287.
- [25] H. Abuki, T. Hatsuda, and K. Itakura, Structural change of Cooper pairs and momentum dependent gap in color superconductivity, *Phys. Rev. D* **65**, 074014 (2002), arXiv:hep-ph/0109013.
- [26] G. Comitini and F. Siringo, QCD phase diagram from the gluon propagator at finite temperature and density, (2024), arXiv:2412.15414 [hep-th].
- [27] J. M. Cornwall, R. Jackiw, and E. Tomboulis, Effective Action for Composite Operators, *Phys. Rev. D* **10**, 2428 (1974).
- [28] D. K. Hong, V. A. Miransky, I. A. Shovkovy, and L. C. R. Wijewardhana, Schwinger-Dyson approach to color superconductivity in dense QCD, *Phys. Rev. D* **61**, 056001 (2000), [Erratum: *Phys.Rev.D* 62, 059903 (2000)], arXiv:hep-ph/9906478.
- [29] D. Müller, M. Buballa, and J. Wambach, Dyson-Schwinger approach to color superconductivity at finite temperature and density, *Eur. Phys. J. A* **49**, 96 (2013), arXiv:1303.2693 [hep-ph].
- [30] D. Müller, M. Buballa, and J. Wambach, Dyson-Schwinger Approach to Color-Superconductivity: Effects of Selfconsistent Gluon Dressing, (2016), arXiv:1603.02865 [hep-ph].
- [31] H. Malekzadeh and D. H. Rischke, Gluon self-energy in the color-flavor-locked phase, *Phys. Rev. D* **73**, 114006 (2006), arXiv:hep-ph/0602082.
- [32] D.-f. Hou, Q. Wang, and D. H. Rischke, Generalized Ward identity and gauge invariance of the color superconducting gap, *Phys. Rev. D* **69**, 071501 (2004), arXiv:hep-ph/0401152.
- [33] G. ’t Hooft, Computation of the quantum effects due to a four-dimensional pseudoparticle, *Phys. Rev. D* **14**, 3432 (1976).
- [34] G. ’t Hooft, How instantons solve the u(1) problem, *Physics Reports* **142**, 357 (1986).
- [35] F. Murgana, D. E. A. Castillo, A. G. Grunfeld, and M. Ruggieri, Topological susceptibility and axion potential in two-flavor superconductive quark matter, *Phys. Rev. D* **110**, 014042 (2024), arXiv:2404.14160 [hep-ph].
- [36] Z. Zhang and W. Zhao, Properties of QCD axion in two-flavor color superconductive matter with massive quarks, (2025), arXiv:2501.04560 [hep-ph].

- [37] R. Balkin, J. Serra, K. Springmann, and A. Weiler, The QCD axion at finite density, *JHEP* **07**, 221, arXiv:2003.04903 [hep-ph].
- [38] R. D. Peccei and H. R. Quinn, Cp conservation in the presence of instantons, *Phys. Rev. Lett.* **38**, 1440 (1977).
- [39] R. D. Peccei and H. R. Quinn, Constraints imposed by cp conservation in the presence of instantons, *Phys. Rev. D* **16**, 1791 (1977).
- [40] F. Wilczek, Problem of strong p and t invariance in the presence of instantons, *Phys. Rev. Lett.* **40**, 279 (1978).
- [41] R. Casalbuoni, Effective description of QCD at high density, *eConf C010815*, 88 (2002), arXiv:hep-ph/0110107.
- [42] D. K. Hong, An Effective field theory of QCD at high density, *Phys. Lett. B* **473**, 118 (2000), arXiv:hep-ph/9812510.
- [43] D. K. Hong, Aspects of high density effective theory in QCD, *Nucl. Phys. B* **582**, 451 (2000), arXiv:hep-ph/9905523.
- [44] R. Casalbuoni, R. Gatto, M. Mannarelli, and G. Nardulli, Effective gluon interactions in the color superconductive phase of two flavor QCD, *Phys. Lett. B* **524**, 144 (2002), arXiv:hep-ph/0107024.
- [45] S. R. Beane, P. F. Bedaque, and M. J. Savage, Meson masses in high density QCD, *Phys. Lett. B* **483**, 131 (2000), arXiv:hep-ph/0002209.
- [46] R. Anglani, M. Mannarelli, and M. Ruggieri, Collective modes in the color flavor locked phase, *New J. Phys.* **13**, 055002 (2011), arXiv:1101.4277 [hep-ph].
- [47] R. Casalbuoni, R. Gatto, M. Mannarelli, and G. Nardulli, Anisotropy parameters for the effective description of crystalline color superconductors, *Phys. Rev. D* **66**, 014006 (2002), arXiv:hep-ph/0201059.
- [48] R. Casalbuoni, R. Gatto, M. Mannarelli, and G. Nardulli, Effective field theory for the crystalline color superconductive phase of QCD, *Phys. Lett. B* **511**, 218 (2001), arXiv:hep-ph/0101326.
- [49] R. Anglani, R. Casalbuoni, M. Ciminale, N. Ippolito, R. Gatto, M. Mannarelli, and M. Ruggieri, Crystalline color superconductors, *Rev. Mod. Phys.* **86**, 509 (2014), arXiv:1302.4264 [hep-ph].
- [50] R. Anglani, G. Nardulli, M. Ruggieri, and M. Mannarelli, Neutrino emission from compact stars and inhomogeneous color superconductivity, *Phys. Rev. D* **74**, 074005 (2006), arXiv:hep-ph/0607341.
- [51] R. Casalbuoni, M. Ciminale, M. Mannarelli, G. Nardulli, M. Ruggieri, and R. Gatto, Effective gap equation for the inhomogeneous LOFF superconductive phase, *Phys. Rev. D* **70**, 054004 (2004), arXiv:hep-ph/0404090.
- [52] R. Casalbuoni, R. Gatto, M. Mannarelli, G. Nardulli, M. Ruggieri, and S. Stramaglia, Quasiparticle specific heats for the crystalline color superconducting phase of QCD, *Phys. Lett. B* **575**, 181 (2003), [Erratum: *Phys.Lett.B* 582, 288–288 (2004)], arXiv:hep-ph/0307335.
- [53] R. Casalbuoni, E. Fabiano, R. Gatto, M. Mannarelli, and G. Nardulli, Phonons and gluons in the crystalline color superconducting phase of QCD, *Phys. Rev. D* **66**, 094006 (2002), arXiv:hep-ph/0208121.
- [54] K. S. Jeong, F. Murgana, A. Dash, and D. H. Rischke, Functional Renormalization Group analysis of the quark-condensation pattern on the Fermi surface: A simple effective-model approach, (2024), arXiv:2407.13589 [nucl-th].
- [55] T. Schäfer and E. V. Shuryak, Instantons in QCD, *Rev. Mod. Phys.* **70**, 323 (1998), arXiv:hep-ph/9610451.
- [56] T. Hell, S. Rossner, M. Cristoforetti, and W. Weise, Thermodynamics of a three-flavor nonlocal Polyakov-Nambu-Jona-Lasinio model, *Phys. Rev. D* **81**, 074034 (2010), arXiv:0911.3510 [hep-ph].
- [57] B. Zhang, D. E. A. Castillo, A. G. Grunfeld, and M. Ruggieri, Exploring the axion potential and axion walls in dense quark matter, *Phys. Rev. D* **108**, 054010 (2023).
- [58] B. S. Lopes, R. L. S. Farias, V. Dexheimer, A. Bandyopadhyay, and R. O. Ramos, Axion effects in the stability of hybrid stars, *Phys. Rev. D* **106**, L121301 (2022), arXiv:2206.01631 [hep-ph].
- [59] A. Bandyopadhyay, R. L. S. Farias, B. S. Lopes, and R. O. Ramos, Quantum chromodynamics axion in a hot and magnetized medium, *Phys. Rev. D* **100**, 076021 (2019), arXiv:1906.09250 [hep-ph].
- [60] R. K. Mohapatra, A. Abhishek, A. Das, and H. Mishra, In medium properties of axion within a polyakov loop enhanced nambu-jona-lasinio model, in *Springer Proc. Phys.*, Vol. 277 (2022) pp. 455–458.
- [61] A. Das, H. Mishra, and R. K. Mohapatra, In medium properties of an axion within a 2+1 flavor polyakov loop enhanced nambu-jona-lasinio model, *Phys. Rev. D* **103**, 074003 (2021), arXiv:2006.15727 [hep-ph].
- [62] H. F. Gong, Q. Lu, Z. Y. Lu, L. M. Liu, X. Chen, and S. P. Wang, Qcd topology and axion properties in an isotropic hot and dense medium (2024), arXiv:2404.15136 [hep-ph].
- [63] D. Kumar and H. Mishra, CP violation in cold dense quark matter and axion effects on the non-radial oscillations of neutron stars, (2024), arXiv:2411.17828 [hep-ph].
- [64] J. Bersini, A. D’Alise, C. Gambardella, and F. San-nino, On the θ -angle physics of QCD under pressure: The strange and isospin phase diagram, (2025), arXiv:2501.04261 [hep-ph].
- [65] R. L. W. et al. [Particle Data Group], Review of particle physics, *PTEP* **2022**, 083C01 (2022).
- [66] G. Gabadadze and M. A. Shifman, Vacuum structure and the axion walls in gluodynamics and qcd with light quarks, *Phys. Rev. D* **62**, 114003 (2000), arXiv:hep-ph/0007345 [hep-ph].
- [67] A. Davidson and M. A. H. Vozmediano, The horizontal axion alternative: The interplay of vacuum structure and flavor interactions, *Nucl. Phys. B* **248**, 647 (1984).
- [68] F. Takahashi, W. Yin, and A. H. Guth, Qcd axion window and low-scale inflation, *Phys. Rev. D* **98**, 015042 (2018), arXiv:1805.08763 [hep-ph].
- [69] A. Davidson and M. A. H. Vozmediano, Domain walls: Horizontal epilogue, *Phys. Lett. B* **141**, 177 (1984).
- [70] T. Schäfer, Instanton effects in QCD at high baryon density, *Phys. Rev. D* **65**, 094033 (2002), arXiv:hep-ph/0201189.
- [71] S. I. Kruglov, Instanton-induced four-quark interactions, *Soviet Physics Journal* **33**, 580 (1990).
- [72] F. Schrempp, Instanton-induced processes: An Overview, in *HERA and the LHC: A Workshop on the Implications of HERA for LHC Physics: CERN - DESY Workshop 2004/2005 (Midterm Meeting, CERN, 11-13 October 2004; Final Meeting, DESY, 17-21 January 2005)* (2005) pp. 3–16, arXiv:hep-ph/0507160.

- [73] E. Shuryak and I. Zahed, Hadronic structure on the light front. I. Instanton effects and quark-antiquark effective potentials, *Phys. Rev. D* **107**, 034023 (2023), arXiv:2110.15927 [hep-ph].
- [74] M. A. Shifman, A. I. Vainshtein, and V. I. Zakharov, Instanton Density in a Theory with Massless Quarks, *Nucl. Phys. B* **163**, 46 (1980).
- [75] D. T. Son, M. A. Stephanov, and A. R. Zhitnitsky, Domain walls of high density QCD, *Phys. Rev. Lett.* **86**, 3955 (2001), arXiv:hep-ph/0012041.
- [76] T. Schäfer, Quark hadron continuity in QCD with one flavor, *Phys. Rev. D* **62**, 094007 (2000), arXiv:hep-ph/0006034.
- [77] R. Casalbuoni, R. Gatto, G. Nardulli, and M. Ruggieri, Aspects of the color flavor locking phase of QCD in the Nambu-Jona Lasinio approximation, *Phys. Rev. D* **68**, 034024 (2003), arXiv:hep-ph/0302077.
- [78] A. Pilaftsis and D. Teresi, Symmetry-Improved 2PI Approach to the Goldstone-Boson IR Problem of the SM Effective Potential, *Nucl. Phys. B* **906**, 381 (2016), arXiv:1511.05347 [hep-ph].
- [79] G. Aarts, D. Ahrensmeier, R. Baier, J. Berges, and J. Serreau, Far from equilibrium dynamics with broken symmetries from the 2PI - $1/N$ expansion, *Phys. Rev. D* **66**, 045008 (2002), arXiv:hep-ph/0201308.
- [80] S. Tsutsui, J.-P. Blaizot, and Y. Hatta, Thermalization of overpopulated systems in the 2PI formalism, *Phys. Rev. D* **96**, 036004 (2017), arXiv:1705.02872 [hep-ph].
- [81] C. Wetterich, Bosonic effective action for interacting fermions, *Phys. Rev. B* **75**, 085102 (2007), arXiv:cond-mat/0208361.
- [82] E. A. Calzetta and B.-L. B. Hu, *Nonequilibrium Quantum Field Theory* (Oxford University Press, 2009).
- [83] J. Berges, Nonequilibrium Quantum Fields: From Cold Atoms to Cosmology, (2015), arXiv:1503.02907 [hep-ph].
- [84] J.-P. Blaizot, J. M. Pawłowski, and U. Reinosa, Functional renormalization group and 2PI effective action formalism, *Annals Phys.* **431**, 168549 (2021), arXiv:2102.13628 [hep-th].
- [85] N. Dupuis, Renormalization group approach to interacting fermion systems in the two-particle-irreducible formalism, *Eur. Phys. J. B* **48**, 319 (2005), arXiv:cond-mat/0506542.
- [86] T. Bode, The two-particle irreducible effective action for classical stochastic processes, *Journal of Physics A: Mathematical and Theoretical* **55**, 265401 (2022).
- [87] J. Goldstone, A. Salam, and S. Weinberg, Broken Symmetries, *Phys. Rev.* **127**, 965 (1962).
- [88] G. Jona-Lasinio, Relativistic field theories with symmetry breaking solutions, *Nuovo Cim.* **34**, 1790 (1964).
- [89] V. G. Bornyakov, V. V. Braguta, A. A. Nikolaev, and R. N. Rogalyov, Effects of dense quark matter on gluon propagators in lattice QC_2D , *Phys. Rev. D* **102**, 114511 (2020).
- [90] V. G. Bornyakov and R. N. Rogalyov, Gluons in two-color QCD at high baryon density, *Int. J. Mod. Phys. A* **36**, 2044032 (2021), <https://doi.org/10.1142/S0217751X20440327>.
- [91] V. G. Bornyakov, A. A. Nikolaev, R. N. Rogalyov, and A. S. Terentev, Gluon propagators in $2+1$ lattice QCD with nonzero isospin chemical potential, *Eur. Phys. J. C* **81**, 747 (2021).
- [92] D. B. Leinweber, J. I. Skullerud, A. G. Williams, and C. Parrinello, Asymptotic scaling and infrared behavior of the gluon propagator, *Phys. Rev. D* **60**, 094507 (1998).
- [93] A. C. Aguilar and A. A. Natale, A dynamical gluon mass solution in a coupled system of the Schwinger-Dyson equations, *Journal of High Energy Physics* **2004**, 057 (2004).
- [94] A. C. Aguilar and J. Papavassiliou, Gluon mass generation in the PT-BFM scheme, *J. High Energy Phys.* **2006** (12), 012.
- [95] I. L. Bogolubsky, E.-M. Ilgenfritz, M. Müller-Preussker, and A. Sternbeck, Lattice gluodynamics computation of Landau-gauge Green's functions in the deep infrared, *Phys. Lett. B* **676**, 69 (2009).
- [96] M. Tissier and N. Wschebor, Infrared propagators of Yang-Mills theory from perturbation theory, *Phys. Rev. D* **82**, 101701 (2010).
- [97] M. Peláez, M. Tissier, and N. Wschebor, Two-point correlation functions of QCD in the Landau gauge, *Phys. Rev. D* **90**, 065031 (2014).
- [98] A. G. Duarte, O. Oliveira, and P. J. Silva, Lattice gluon and ghost propagators, and the strong coupling in pure $SU(3)$ Yang-Mills theory: Finite lattice spacing and volume effects, *Phys. Rev. D* **94**, 014502 (2016).
- [99] U. Reinosa, J. Serreau, M. Tissier, and N. Wschebor, How nonperturbative is the infrared regime of Landau gauge Yang-Mills correlators?, *Phys. Rev. D* **96**, 014005 (2017).
- [100] M. Napetschnig, R. Alkofer, M. Q. Huber, and J. M. Pawłowski, Yang-Mills propagators in linear covariant gauges from Nielsen identities, *Phys. Rev. D* **104**, 054003 (2021).
- [101] D. Dudal, J. A. Gracey, S. P. Sorella, N. Vandersickel, and H. Verschelde, Refinement of the Gribov-Zwanziger approach in the Landau gauge: Infrared propagators in harmony with the lattice results, *Phys. Rev. D* **78**, 065047 (2008).
- [102] D. Dudal, O. Oliveira, and N. Vandersickel, Indirect lattice evidence for the refined Gribov-Zwanziger formalism and the gluon condensate $\langle A^2 \rangle$ in the Landau gauge, *Phys. Rev. D* **81**, 074505 (2010).
- [103] G. Comitini, T. De Meerleer, D. Dudal, and S. P. Sorella, Dynamically massive linear covariant gauges: Setup and first results, *Phys. Rev. D* **109**, 014037 (2024).
- [104] F. Siringo, Analytical study of Yang-Mills theory in the infrared from first principles, *Nucl. Phys. B* **907**, 572 (2016).
- [105] F. Siringo, Analytic structure of QCD propagators in Minkowski space, *Phys. Rev. D* **94**, 114036 (2016).
- [106] F. Siringo and G. Comitini, The gluon propagator in linear covariant R_ξ gauges, *Phys. Rev. D* **98**, 034023 (2018).
- [107] G. Comitini and F. Siringo, One-loop RG improvement of the screened massive expansion in the Landau gauge, *Phys. Rev. D* **102**, 094002 (2020).
- [108] H. Abuki, T. Hatsuda, and K. Itakura, Color superconductivity in dense QCD and structure of cooper pairs, in *Joint CSSM / JHF / NITP Workshop on Physics at the Japan Hadron Facility* (2002) arXiv:hep-ph/0206043.
- [109] S. B. Ruester, V. Werth, M. Buballa, I. A. Shovkovy, and D. H. Rischke, The phase diagram of neutral quark matter: Self-consistent treatment of quark masses,

- Phys. Rev. D **72**, 034004 (2005), arXiv:hep-ph/0503184 [hep-ph].
- [110] S. N. et al. (Particle Data Group), Review of particle physics, Phys. Rev. D **110**, 030001 (2024).
- [111] L. D. Luzio, M. Fedele, M. Giannotti, F. Mescia, and E. Nardi, Stellar evolution confronts axion models, Journal of Cosmology and Astroparticle Physics **2021** (11), 073, arXiv:2109.10368 [hep-ph].
- [112] P. Carenza, M. Giannotti, J. Isern, A. Mirizzi, and O. Straniero, Axion astrophysics, Physics Reports **1000**, 1 (2024), arXiv:2411.02492 [hep-ph].